

PACS 73.40.-c, 73.61.Ga, 78.30.Fs

## **Injection current and infrared photosensitivity in isotype $p$ -PbTe/ $p$ -CdTe heterojunctions**

**V.V. Tetyorkin<sup>1</sup>, A.V. Sukach<sup>1</sup>, A.I. Tkachuk<sup>2</sup> and S.P. Movchan<sup>1</sup>**

<sup>1</sup>*V. Lashkaryov Institute of Semiconductor Physics, National Academy of Sciences of Ukraine, 45, prospect Nauky, 03028 Kyiv, Ukraine*

<sup>2</sup>*V. Vinnichenko Kirovograd State Pedagogical University, Kirovograd, Ukraine*  
Phone: 38 (044) 525-1813; e-mail: teterkin@isp.kiev.ua

**Abstract.** Iso-type  $p$ -PbTe/ $p$ -CdTe heterojunctions were grown on BaF<sub>2</sub> substrates by using the hot-wall epitaxy technique. The growth details are presented. The carrier transport mechanism was investigated by means of the current-voltage measurements. At 77 K the dominant conduction mechanism was found to be the space-charge-limited current. The photovoltaic response in the long-wave infrared region with the half-peak cut-off wavelength ranged from 8.0 to 9.0  $\mu\text{m}$  was observed in these heterojunctions for the first time. The possible mechanism of the photoresponse is the internal photoemission of holes from  $p$ -PbTe across the heterojunction barrier.

**Keywords:** iso-type, heterojunction, infrared, photovoltaic, response.

Manuscript received 25.10.12; revised version received 00.00.12; accepted for publication 00.00.12; published online 00.00.12.

### **1. Introduction**

PbTe/CdTe heterostructures are of great interest from both scientific and applied points of view. PbTe is a narrow-gap semiconductor that is widely used to manufacture mid-wavelength infrared lasers and detectors [1-3]. It is also known as important material for thermoelectric applications. Increased values of the thermoelectric efficiency in PbTe-based devices are expected to be obtained in low-dimensional quantum structures, like superlattices and quantum dot systems [4, 5]. CdTe is very important material for application in solar cells, X-ray and  $\gamma$ -ray detectors [5, 6]. Their physical parameters (band gap, static dielectric constant, effective masses of carriers, etc.) differ significantly, so unusual physical phenomena are expected in heterostructures based on these semiconductors. Recently, structural and energetic properties of PbTe/CdTe (100), (110) and (111) interfaces were investigated theoretically. The results yield the type-I character of PbTe/CdTe heterostructures. The valence

band offset (VBO) was calculated by Leitsmann et al. within the density functional theory in local density approximation [7, 8]. It has been shown that the PbTe/CdTe (111) interface is the most energetically stable. Only a weak dependence of the VBO on the interface orientation was found. The calculated values of VBO were 0.37 and 0.42 eV for the polar (100) and nonpolar (110) interfaces, when the spin-orbit interaction was not taken into account. By adding this interaction, the VBO was close to zero. Using a tight-binding model the VBO equal to 0.19 eV was obtained by Buřala et al. for PbTe/CdTe (110) interface [9]. In this calculation, the spin-orbit interaction was included. The values of the VBO 0.135 $\pm$ 0.05 and 0.09 $\pm$ 0.12 eV were experimentally determined using X-ray and ultraviolet photoelectron spectroscopy measurements, respectively [10, 11]. To our knowledge, investigations of physical properties of iso-type  $p$ -PbTe/ $p$ -CdTe heterostructures were not reported in literature. The aim of this investigation is to clarify their transport and photoelectric properties.

## 2. Experimental

The iso-type  $p$ -PbTe/ $p$ -CdTe heterojunctions were grown on cleaved (111) BaF<sub>2</sub> substrates using a hot-wall epitaxy (HWE) technique [12, 13]. The most important advantage of HWE is the growth under near equilibrium conditions. Also, it must be pointed out that evaporation of both semiconductors is congruent. This results in epitaxial layers of high quality. The experimental set-up was equipped by two evaporators, each charged with a source material for successive growth of epitaxial layers. The starting materials were single crystals of CdTe and PbTe of the  $p$ -type conductivity and grown by the Bridgman technique. The hole concentration  $p = (8...10) \cdot 10^{15} \text{ cm}^{-3}$  and mobility of the order of  $80 \text{ cm}^2 \text{ V}^{-1} \text{ s}^{-1}$  were measured in  $p$ -CdTe at room temperature. The hole concentration in the initial  $p$ -PbTe was  $4 \cdot 10^{17} \text{ cm}^{-3}$ .

To prepare the heterojunctions, the growth conditions were optimized by studying electrical parameters of PbTe and CdTe epitaxial layers grown on BaF<sub>2</sub> for different substrate and source temperatures. The best results were obtained for the following growth conditions:  $T_{\text{substr}} = 380 \text{ }^\circ\text{C}$ ,  $T_{\text{wall}} = 480 \text{ }^\circ\text{C}$ ,  $T_{\text{source}} = 420 \text{ }^\circ\text{C}$  for PbTe and  $T_{\text{substr}} = 280 \text{ }^\circ\text{C}$ ,  $T_{\text{wall}} = 400 \text{ }^\circ\text{C}$ ,  $T_{\text{source}} = 360 \text{ }^\circ\text{C}$  for CdTe. Also, buffer layers of PbTe with the thickness of the order of  $1.0 \text{ } \mu\text{m}$  were previously grown on freshly cleaved substrates. After that, PbTe and CdTe layers were sequentially grown using a stainless steel mask that delineated a circular area of  $1.7 \cdot 10^{-2} \text{ cm}^2$ . So, the total thickness of PbTe epitaxial layers was close to  $1.5 \text{ } \mu\text{m}$ , whereas the thickness of CdTe layers was ranged from  $0.4$  to  $4.0 \text{ } \mu\text{m}$ . The hole concentration  $(2...6) \cdot 10^{17} \text{ cm}^{-3}$  and mobility of the order of  $3 \cdot 10^3 \text{ cm}^2 \text{ V}^{-1} \text{ s}^{-1}$  was measured in the buffer layers at  $77 \text{ K}$ . CdTe layers grown on BaF<sub>2</sub> substrates had the specific resistance of the order of  $10^5 \text{ Ohm}\cdot\text{cm}$ . Because of Hall measurements were not feasible at  $77 \text{ K}$ , the hole concentration was estimated from the capacitance-voltage measurements in Au/ $p$ -CdTe Schottky contacts. The contacts were prepared by electrolytic deposition of Au on as-grown epitaxial layers. They were characterized by the potential barrier height of the order of  $0.5\text{-}0.6 \text{ eV}$ . The concentration of holes close to  $1 \cdot 10^{13} \text{ cm}^{-3}$  was determined from the slope of  $C^{-2} - U$  dependences. Ohmic contacts to CdTe were prepared by evaporation of Au in a vacuum chamber, followed by half an hour thermal annealing in H<sub>2</sub> atmosphere at  $180 \text{ }^\circ\text{C}$ . Ohmic contacts to  $p$ -PbTe were soldered using Sn - Au alloy.

## 3. Results and discussion

The heterojunctions were studied by the capacitance-voltage, current-voltage and photoresponse

measurements at temperature  $77 \text{ K}$ . The junction capacitance was measured using  $1 \text{ MHz}$  testing signal. It should be pointed out that the specific resistance of  $p$ -CdTe layers  $\sim 10^5 \text{ Ohm}\cdot\text{cm}$  results in the dielectric relaxation time  $\tau = \rho \epsilon_0 \epsilon$  of the order of  $\sim 10^{-7} \text{ s}$  for the value of the permittivity of CdTe  $\epsilon = 10$  [5, 6]. This indicates that holes can respond to the testing signal. The measured capacitance was found to be independent on the polarity of the applied bias within the voltage range  $\pm 2.0 \text{ V}$ . Its magnitude was close to the geometric capacitance of CdTe layer. Also, this result indicates that the surface states do not affect the junction capacitance.

At room temperature ohmic  $I - U$  characteristics were observed in the most investigated heterojunctions, irrespective of the polarity of applied bias. This result is important for manufacturing the ohmic contacts to CdTe and will be analyzed in details elsewhere. At the temperature  $T = 77 \text{ K}$ , the current-voltage characteristics had asymmetrical diode-type form with the forward direction corresponding to the negative potential on the CdTe side of a heterojunction. Fig. 1 shows typical dependences of the forward and reverse current on the applied bias measured in a representative heterojunction. In Fig. 2, the forward current-voltage characteristics of three heterojunctions with different thicknesses of CdTe are shown in log-log coordinates. As seen, at low bias voltages an ohmic region,  $I \sim U$ , is observed, followed by a square-law region at higher biases. The crossover voltage,  $U_x$ , at which transition from the first to the second region occurs, shifts towards higher voltages with increase in the thickness of CdTe. In the most investigated heterojunctions, the reverse current was approximated by a power law  $I \sim U^m$  with the exponent  $m = 1.1 - 1.3$ .

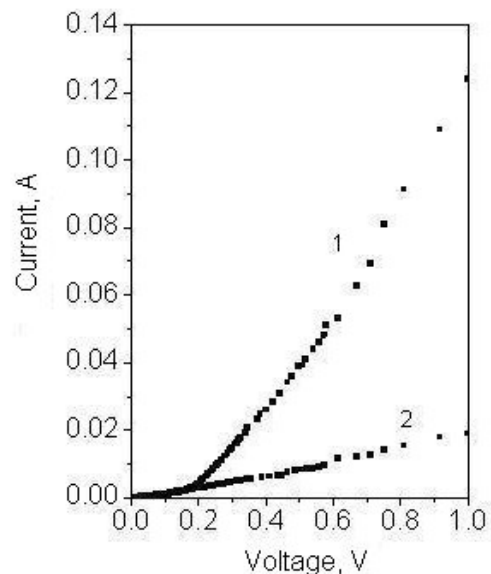


**Fig. 1.** Forward (1) and reverse (2) currents vs bias voltage in a heterojunction with the thickness of CdTe layer equal to  $0.4 \text{ } \mu\text{m}$ . The forward current corresponds to the negative potential on CdTe.

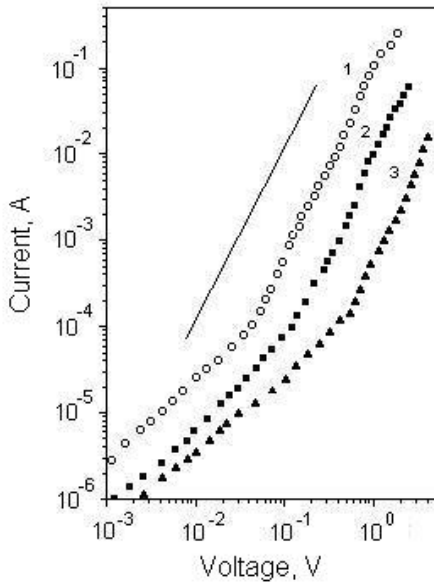


**Fig. 2.** Current-voltage characteristics of three heterojunctions with the thickness of CdTe layer 0.4 (1), 1.4 (2) and 2.8 (3)  $\mu\text{m}$ , respectively. The solid line represents the calculated SCLC according to the formula (2).

The above features of the current-voltage characteristics are in accordance with Lampert's theory of the space-charge-limited current (SCLC) [14]. In the investigated heterojunctions, holes may be injected from the narrow-gap PbTe to the wide-gap CdTe across a potential barrier at the interface. At low biases, the current-voltage dependence is expressed as

$$I = qp_0 \mu \frac{U}{L}, \quad (1)$$

where  $p_0$  is the concentration of thermally generated holes in CdTe. In the simplest case of trap-free sample, the injection current is given by

$$I = \frac{9}{8} \varepsilon_0 \varepsilon \mu \frac{U^2}{L^3}, \quad (2)$$

also known as the Mott-Garney square law [14]. In the latter equation,  $\mu$  is the drift mobility of holes,  $\varepsilon_0$  – permittivity of vacuum and  $\varepsilon$  – static dielectric constant of CdTe,  $L$  – the thickness of CdTe layer and  $U$  – applied bias voltage. As seen from Fig. 2, there is pronounced difference between the measured and calculated data, which can be attributed to capture of holes to traps in CdTe. In the case of a single trap level, the current-voltage characteristic is given by [14]

$$I = \frac{9}{8} \varepsilon_0 \varepsilon \mu \Theta \frac{U^2}{L^3}, \quad (3)$$

where the constant  $\Theta$  represents the ratio of free to trapped holes. The crossover voltage in this case is determined as

$$U_x = \frac{qp_0 L^2}{\varepsilon_0 \varepsilon \Theta}. \quad (4)$$

To calculate the ohmic current, the concentration of holes was assumed to be the same as in CdTe layers grown on  $\text{BaF}_2$  substrates. By considering the hole mobility as a fitting parameter, the coincidence between the calculated and measured data was obtained for the values of the hole mobility 5-10  $\text{cm}^2\text{V}^{-1}\text{s}^{-1}$ .

Previously the SCLC in CdTe-based structures was investigated in several papers. The SCLC in  $n$ -GaAs/CdTe heterostructures was assumed to be caused by injection of electrons from  $n$ -GaAs and their capture by defect states in semi-insulating CdTe [15]. The injection of carriers from contacts was observed in CdTe single crystals and polycrystalline films of  $n$ - and  $p$ -type conductivity [16-21]. The SCLC in these investigations was analyzed by the single-carrier injection mechanism.

The most important feature of the investigated heterojunctions is the existence of photovoltaic response in the long-wave infrared region. The normalized photoresponse spectra measured for two illumination geometries in the open-circuit mode are shown in Fig. 3. As seen, both spectra consist of two spectral bands with the half-peak cut-off wavelength  $\lambda_{c1} \cong 5.8 \mu\text{m}$  and  $\lambda_{c2} \cong 8.0 - 9.0 \mu\text{m}$ , respectively. The important fact is that the polarity of the measured photocurrent is not changed within the whole spectral range. Moreover, the photocurrent was found to increase, when negative potential was applied to CdTe. Note that the investigated heterojunctions exhibited the photovoltaic response in the spectral region where both heterojunction constituents are not sensitive.

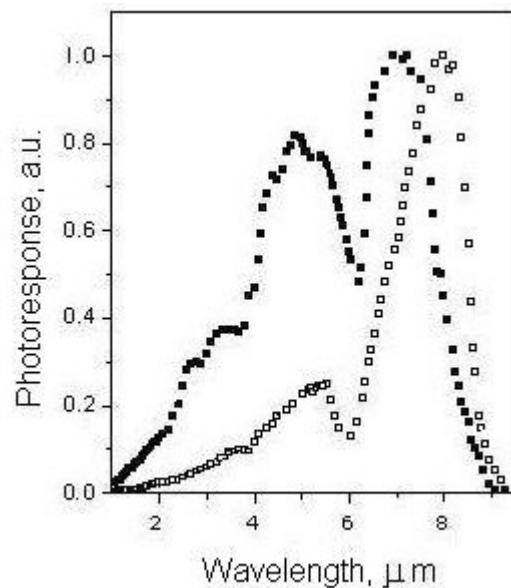


**Fig. 3.** Spectral dependences of the photovoltaic response in a heterojunction illuminated from PbTe (open dots) and CdTe (close dots) sides, respectively

Previously, the photovoltaic response at energies lower than the band gap of Ge and Si constituents was observed in iso-type  $n$ -Ge/ $n$ -Si heterojunctions that were characterized by large density of interface states [22]. The band diagram of these heterojunctions was represented by a model of double Schottky barriers. The experimentally observed change of sign of the photoresponse in  $n$ -Ge/ $n$ -Si heterojunctions was explained by excitation of electrons from the interface states. In the investigated PbTe/CdTe heterojunctions, the sign of the photoresponse was not changed. It is most likely that in this case the interband excitation of electron-hole pairs in PbTe and photoemission of free holes from PbTe across the heterojunction are dominant mechanisms of the photoresponse. At short wavelengths, both mechanisms can contribute to the photoresponse, whereas at longer wavelength only internal photoemission of holes is possible. This results in two spectral bands of the photoresponse. The cut-off wavelength  $\lambda_{c1}$  can be attributed to the energy gap of PbTe. The internal photoemission is well investigated in iso-type  $p^+$ -Ge<sub>x</sub>Si<sub>1-x</sub>/ $p$ -Si heterojunctions [2]. It has been shown that the long-wavelength edge of the photoresponse in these structures depends on the VBO and the Fermi level position in  $p^+$ -Ge<sub>x</sub>Si<sub>1-x</sub>. Using the known band parameters of PbTe [1], the Fermi level in  $p$ -PbTe was estimated to lie below the valence band edge at a distance less than 10 meV. So, it may be concluded that the cut-off wavelength  $\lambda_{c2}$  is mainly determined by the VBO, and its value is ranged from 0.14 to 0.16 eV. Obviously, further verification of the model of internal photoemission can be achieved by doping of lead telluride. These experiments are in progress now.

As seen from Fig. 3, the measured spectrum is broader in the case when the heterojunction is illuminated from the CdTe side. This effect may be explained by more effective collection of mobile holes, which are excited by radiation in the immediate vicinity to the heterojunction. Finally, the band bending in CdTe was estimated to be 0.065...0.085 eV for the hole concentration of the order of  $10^{13} \text{ cm}^{-3}$  and the effective mass of holes equal to  $0.35m_0$  [5].

#### 4. Conclusions

Iso-type  $p$ -PbTe/ $p$ -CdTe heterojunctions were grown on BaF<sub>2</sub> by HWE technique. The dark current at 77 K is explained by injection of holes from highly doped  $p$ -PbTe to high resistance  $p$ -CdTe. The long-wavelength photovoltaic response at 77 K is explained by internal photoemission of holes from  $p$ -PbTe across the heterojunction barrier. The cut-off wavelength of the photoresponse is determined by the VBO. The value of the VBO 0.14...0.16 eV found in this study is in

agreement with theoretically predicted and experimentally measured data.

#### References

1. G. Nimitz and B. Schlicht, Narrow-gap lead salts, in: R. Dornhaus, G. Nimitz and B. Schlicht (Eds.), *Narrow-Gap Semiconductors*. Springer, Berlin, 1985.
2. A. Rogalski, IV-VI Detectors, in: *Infrared Photon Detectors*, A. Rogalski (Ed.). SPIE Optical Engineering Press, Bellingham, 1995.
3. M. Rahim, M. Arnold, F. Felder, K. Behfar, and H. Zogg, Midinfrared lead-chalcogenide vertical external cavity surface emitting laser with 5  $\mu\text{m}$  wavelength // *Appl. Phys. Lett.* **91**(15), p. 151102-1 - 151102-3 (2007).
4. T.C. Harman, P.J. Taylor, M.P. Walsh, B.E. La Forge, Nanostructured thermoelectric materials // *J. Electron. Mater.*, **34** (5), p. L19-L22 (2005).
5. R. Triboulet and P. Siffert, *CdTe and Related Compounds. Physics, Defects, Hetero- and Nanostructures, Crystal Growth Surfaces and Applications*. Oxford, Elsevier, 2010.
6. K. Zanio, Cadmium telluride, in: R.K. Willardson and A.C. Beer (Eds.), *Semiconductors and Semimetals*, vol. 13. Academic Press, New York and London (1978).
7. R. Leitsmann, L.E. Ramos and F. Bechstedt, Structural properties of PbTe/CdTe interfaces from first principles // *Phys. Rev. B*, **74**, p. 085309-1 - 085309-8 (2006).
8. R. Leitsmann and F. Bechstedt, Electronic-structure calculations for polar lattice-structure-mismatched interfaces PbTe/CdTe (100) // *Phys. Rev. B*, **76**, p. 125315-1 - 125315-11 (2007).
9. M. Bukala, P. Sankowski, R. Buczko and P. Kacman, Crystal and electronic structure of PbTe/CdTe nanostructures // *Nanoscale Res. Lett.* **6**, p. 126 (2011).
10. J. Si, S. Jin, H. Zhang, P. Zhu, D. Qiu, H. Wu, Experimental determination of valence band offset at PbTe/CdTe(111) heterojunction interface by x-ray photoelectron spectroscopy // *Appl. Phys. Lett.* **93**(20), p. 202101-1 - 202101-3 (2008).
11. C.F. Cai, H.Z. Wu, J.X. Si et al., Energy band alignment of PbTe/CdTe(111) interface determined by ultraviolet photoelectron spectra using synchrotron radiation // *Chin. Phys. B*, **19**(7), p. 077301-1 - 077301-3 (2010).
12. A Lopez-Otero, Hot wall epitaxy // *Thin Solid Films*, **49** (1), p. 3-57 (1978).
13. H. Clemens, E.J. Fantner, G. Bauer, Hot-wall epitaxy system for the growth of multilayer IV-VI compound heterostructures // *Rev. Sci. Instrum.* **54**, p. 685-689 (1983).
14. M.A. Lampert, P. Mark, *Current Injection in Solids*. Academic Press, New York, 1970.

15. Madan Niraula, Toru Aoki, Yoichiro Nakanishi, and Yoshinori Hatanaka, Radical assisted metalorganic chemical vapor deposition of CgTe on GaAs and carrier transport mechanism in CdTe/n-GaAs heterojunction // *J. Appl. Phys.* **83**(5), p. 2656-2661 (1998).
16. A. Zoul, E. Klier, Space charge limited current in high resistivity CdTe crystals // *Czech. J. Phys.* **27**(7), p. 789-796 (1977).
17. X. Mathew, J. Pantoja Enriquez, P.J. Sebastian, M. Pattabi, A. Sanchez-Juarez, J. Campos, J.C. McClure, V.P. Singh, Charge transport mechanism in a typical Au/CdTe Schottky diode // *Solar Energy Mater. & Solar Cells*, **63**(4), p. 355-365 (2000).
18. A.M. Mancini, C. Manfredotti, C. De Blasi, G. Micocci and A. Tepore, Characterization of CdTe with photoelectronic techniques // *Rev. Phys. Appl.* **12**(2), pp. 255-261 (1977).
19. M.G. Mahesha, V.B. Kasturi and G.K. Shivakumar, Characterization of thin film Al/p-CdTe Schottky diode // *Turk. J. Phys.* **32**, p. 151-156 (2008).
20. A. Subbarayan, K. Natarajan S. Lalitha, R. Sathyamoorthy, S. Senthilarasu, Characterization of CdTe thin film – dependence of structural and optical properties on temperature and thickness // *Solar Energy Mater. & Solar Cells*, **82**(1-2), p. 187-199 (2004).
21. K. Mochizuki, K. Masumoto, *I-V* characteristics of CdTe single crystals // *Mater. Lett.* **4**(5-7), p. 301-303 (1986).
22. B.L. Sharma, R.P. Purohit, *Semiconductor Heterojunctions*. Pergamon Press, New York, 1974.